EPJ AP
Applied Physics
EPJ.org
your physics journal

Eur. Phys. J. Appl. Phys. (2013) 61: 30101 DOI: 10.1051/epjap/2013120216

Nickel on porous silicon MSM photo-detector and quantum confinement in nanocrystallites structure as methods to reduce dark current

Mokhtar Zerdali, F. Bechiri, I. Rahmoun, M. Adnane, T. Sahraoui, and S. Hamzaoui

edp sciences

The title "The European Physical Journal" is a joint property of EDP Sciences, Società Italiana di Fisica (SIF) and Springer

Eur. Phys. J. Appl. Phys. (2013) 61: 30101
DOI: 10.1051/epjap/2013120216

THE EUROPEAN PHYSICAL JOURNAL APPLIED PHYSICS

Regular Article

Nickel on porous silicon MSM photo-detector and quantum confinement in nanocrystallites structure as methods to reduce dark current

Mokhtar Zerdali[a], F. Bechiri, I. Rahmoun, M. Adnane, T. Sahraoui, and S. Hamzaoui

Laboratoire de Microscopie Electronique & Sciences des Matériaux (LME&SM), Université des Sciences et de la Technologie d'Oran (USTO), BP 1505, El MNaouer 31100, Usto, Oran, Algeria

Received: 6 June 2012 / Received in final form: 9 October 2012 / Accepted: 14 January 2013
Published online: 8 March 2013 –

Abstract. We propose in this work, contact Schottky Nickel/porous silicon (PSi) system, coupled to nanocrystallites size variation of material for a possible technique to reduce dark current. The device consists of metal- semiconductor-metal photodiode (MSM-PD). Higher barrier Φ_B enhances the performance of MSM-PD through reduction in dark current (Is), and benefits to resolve noise from signal detection of the devices. In order to reduce much more Is, we proposed different anodization times (5–7–10 min) as method to tune the size of nanocrystallites. As result Is value was reduced to almost two orders of magnitude for 10 min etching time, and the value of Is $\approx 10^{-10}$ A. Φ_B reached the value of 0.882 eV. Among the hypothesis suggested in the reduction of Is was the quantum confinement effects. According to Rhoderick model, the Schottky barrier height is explicitly linked to the band gap energy due to the presence of interface states. The existence of narrow nanocrystallites increased energy band gap of PSi and the Schottky barrier height, which in turn reduces Is. The photoluminescence measurements confirmed our hypothesis. Photosensitivity of the device was established by adopting the MSM configuration, and strong absorption was detected in visible range.

1 Introduction

Porous silicon PSi had attracted many researchers in recent years, and was extensively studied in the early 1990s, in view of its application in silicon-based devices for optoelectronic integrated devices. Porous silicon films are compatible with conventional microelectronics technologies which make them very attractive for applications, such as light-emitting diodes [1,2]. It is used as a light trapping layer to increase the efficiency of the solar cell [3,4], and active absorber layer for solar cells, as well as photo-detection [5,6]. Porous silicon had interesting physical properties, such as a wide energy band gap which can be modulated by the size of the nanocrystallites [7]. This latter advantage is used for detection of the entire visible spectrum [8].

Several techniques have been reported to reduce the dark current. Some of them consist in depositing a passivation coating on the entire active area, which reduces the surface conduction charging interface states [9]. The use of a metal pattern on a very thin insulating layer, for obtaining a barrier effect reduces the emission of the thermionic current [10].

To make devices MSM-PD perform, it is important to realize a Schottky barrier high enough to make the dark current as low as possible [11]. It was suggested to increase the Schottky barrier, using noble metals such as palladium (Pd), gold (Au) and platinum (Pt) and nickel (Ni) [12].

In this work, a nickel metal electrode to make Schottky contacts, also due to its high work function, was proposed. Materials with a low work function may not provide enough low dark current when the photo-detector is used in the visible spectrum.

The MSM-PD device was fabricated using the PSi film as an absorbing layer characterized by low dark current. A low-cost structure was proposed from nanocrystalline silicon realized by anodic etching.

Obtaining low dark current was the result of the quantum properties of the MSM-PD structure diodes. The dark current was explicitly controlled by the barrier height at the interface Ni/PSi, which in turn is proportional to the energy band gap of porous silicon. The quantum effects are due to the modulation of the energy band gap. This is generally true in the case where the Fermi level is pinned by interface states to the value of Φ_0 above a valence band [13].

[a] e-mail: mokhtarzerdali@gmail.com

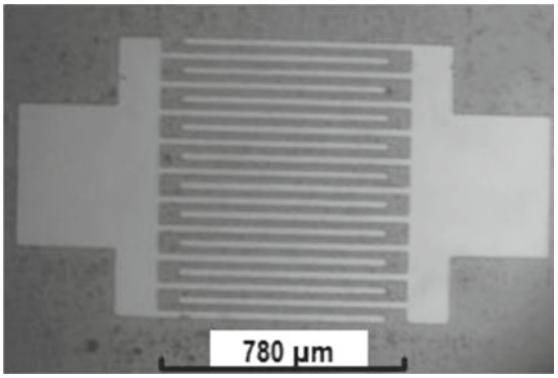

Fig. 1. MSM interdigitated photo-detector based on PSi film. Pitch is of 20 μm.

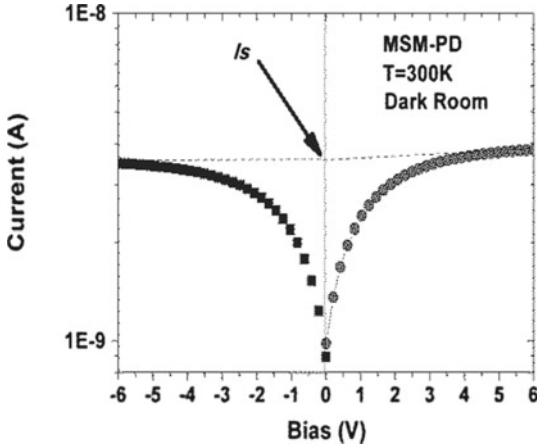

Fig. 2. *I-V* characteristic of planar MSM-PD back-to-back Schottky contacts for Ni/PSi/Ni system.

2 Experimental

The porous silicon PSi films were prepared by anodic etching of a silicon wafer *n*-type, orientation (1 0 0), and a thickness of 150 μm. The plate had a resistivity of 1–2 Ω cm. The silicon was used as an anode while the cathode was of molybdenum foil. The electrolyte was composed of a mixture of ethanol C_2H_5OH, and HF diluted with low concentration of 1%, 2:1 by volume. The silicon surface was etched with a current density of 1 mA/cm^2 for 5 min under exposure to incandescent light (Osram, 24 V/250 W).

Homemade photolithography was performed to develop a commercial photoresist KF1156. The process MSM-PD was supplemented by a metal frame Ni interdigitated electrodes deposited on the front side of the PSi thin film. The deposition was performed by RF sputtering (ULVAC RFS-200) in an argon atmosphere for 10 min and 80 Watts of RF power.

Figure 1 shows the structure of the MSM-PD configuration fabricated by planar interdigitated Schottky contacts characterized by 10 pairs of fingers. The width of a finger and the finger spacing were 20 μm with a lap length of about 600 μm.

The morphological structure of PSi films surface was observed by scanning electron microscopy (SEM-S2500C Hitachi). Advantest TR8652 digital electrometer was connected to record the *I-V* characteristics. Measurements of photoconductivity were performed using a 50 W halogen lamp, and coupled to a plurality of optical interference filters for monochromatic sources. The photoluminescence spectra PL PSi films were examined at room temperature. Photoexcitation of the photoluminescence was obtained thanks to a He-Cd laser 325 nm incident power of 22.3 mW/cm^2. Hamamatsu Photonics spectrophotometer and a multi-channel analyzer C10027 as detector were connected to the system to record the response spectrum in the range of 350–1100 nm.

3 Results and discussions

The performance of the MSM-PD photo-detector depends mainly on the Schottky contacts. Thus it is necessary to determine the Schottky barrier height Φ_B (eV) of the contact, a component of the photodetector planar MSM-PD device.

This, we considered both the photodetector and the MSM-PD configuration classical Ni/PSi/c-Si. The conventional structure was characterized by the deposition of metal film entirely over the PSi thin films [14]. This consideration was taken for the purpose of extracting more precisely the value of Φ_B (eV) from both configurations.

The experimental semi-log(I) vs. V plot was performed for both configurations to determine the barrier height Φ_B. Φ_B is usually calculated from the saturation current determined by extrapolating the curve semi-log(I) vs. V to $V = 0$V, using equation (1) [15].

$$I = I\mathrm{s}\ \mathrm{e}^{qV/nkT}(1 - \mathrm{e}^{-qV/kT}). \tag{1}$$

Here I is the current intensity, k is the Boltzmann constant, T(K) is the temperature, n is the ideality factor, and V is the bias voltage. The Φ_B was calculated from Is according to:

$$I\mathrm{s} = AA^*T^2\mathrm{e}^{-q\Phi B/kT}, \tag{2}$$

and,

$$\Phi_B = kT/q\ln(AA^*T^2/I\mathrm{s}), \tag{3}$$

where A is the area of the diode, A^* is the Richardson constant 110–120 A/cm^2 [16], and q is the electron charge of 1.6×10^{-19} C.

Figure 2 shows a plot of experimental curve log (I) vs. V for MSM-PD device in which only the reverse current can be measured. MSM-PD consists essentially of two Schottky contacts connected back-to-back. When a bias is applied, one of the Schottky contacts is forward biased and the other is reverse biased.

The *I-V* characteristic is fairly symmetrical on both sides confirming a barrier of the same height on the MSM-PD device.

The extrapolation of the curve log(I) at $V = 0$ V for both forward and reverse branches (Fig. 2) intercepts the value of the saturation current Is = 3.5 to 10^{-9} A.

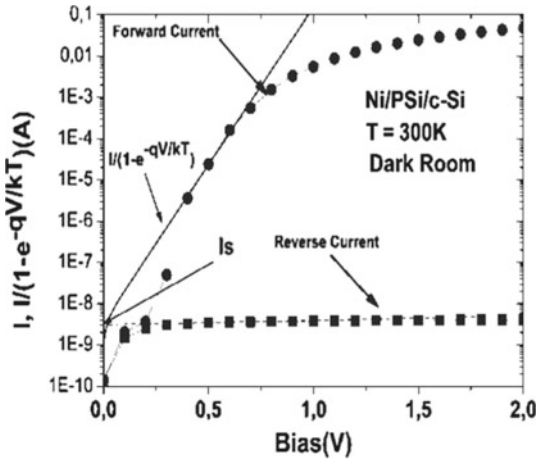

Fig. 3. Semi-log (I) vs. V plot of conventional Ni/PSi/c-Si Schottky diode in reverse and forward branch.

Φ_{B} value of the Schottky contact was calculated from equation (3), and was estimated to be 0.795 eV.

A barrier height of 0.740 eV at 300 K [17], lower than the MSM configuration, was reported for the structure Ni/c-Si (n). The presence of high barrier Φ_{B} further reduces dark current Is, and improves the performance of the MSM-PD device.

Figure 3 shows, however, the shape of the curve log (I) vs. V plot for the structure Ni/PSi/c-Si. The bias contacts were taken of front and rear side of the diode. The extrapolation to $V = 0$ V at both the inverse and direct branch using equation (1) gives $I\mathrm{s} \approx 3.110^{-9}$ A, and $\Phi_{\mathrm{B}} = 0.793$ eV.

Both configurations MSM-PD (Ni/PSi/Ni) and Ni/PSi/c-Si confirm identical barrier height between the metal layer and Ni/PSi, for zero bias V ($V = 0$ V).

Direct current measurements were implemented in small voltage ranges $V \leq 0.7$ V as shown in Figure 3. The I-V characteristics strongly deviate from linearity for $V \geq 0.7$ V due to the effect of the series resistance Rs. The I-V curve quickly becomes dominated by the Rs.

Φ_{B} is given by equation (3), and does not include the Rs. Given the series resistance Rs, the I-V relationship is usually written [18] as:

$$I = I\mathrm{s}\ \mathrm{e}^{q(V-IR\mathrm{s})/(nkT)}(1 - \mathrm{e}^{-q(V-IR\mathrm{s})/(kT)}), \qquad (4)$$

where Is is the saturation current, Rs is the series resistance of the diode, k is the Boltzmann constant, T(K) is the absolute temperature, n is the ideality factor, and V is the bias voltage.

Thus, the parameters of the diode as Φ_{B}, the ideality factor n and Rs were determined by the method proposed by Cheung-Cheung in the nonlinear region [19], expressing equation (4) as functions of Cheung:

$$\mathrm{d}V/\mathrm{d}\ln(I) = n(kT/q) + IR\mathrm{s}, \qquad (5)$$

$$H(I) = V + n(kT/q)\ln(I/AA^{*}T^{2}), \qquad (6)$$

$$H(I) = n\Phi_{B} + IR\mathrm{s}. \qquad (7)$$

Figure 4 shows the experimental curve $\mathrm{d}V/\mathrm{d}\ln(I)$ vs. I plot of the Ni/ PSi/c-Si structure. Using equation (5),

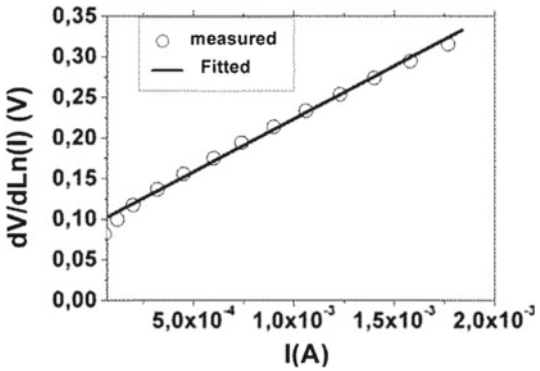

Fig. 4. The $\mathrm{d}V/\mathrm{d}\ln(I)$ vs. I plot of Ni/PSi/c-Si Schottky diode at the temperature of 300 K, in dark room.

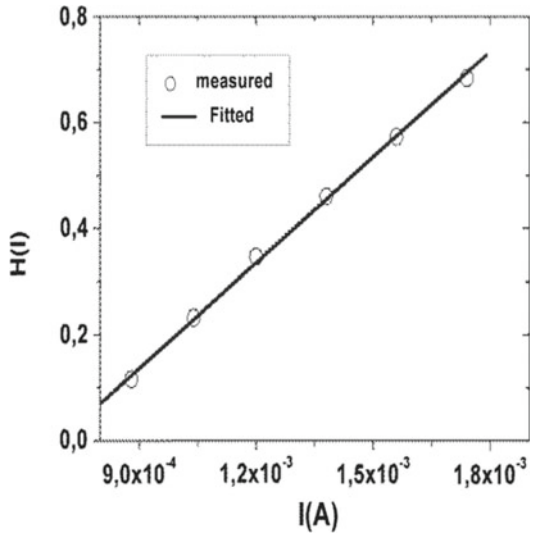

Fig. 5. The $H(I)$ vs. I plot of Ni/PSi/c-Si Schottky diode at the temperature of 300 K, in dark room.

n and Rs may be determined from the intercept of the slope of the line. The value of n and the I-V characteristic data are used to define $H(I)$ using equation (6). The plot of $H(I)$ is a straight line as shown in Figure 5. According to equation (7) the intersection of the slope of this line with the axis gives a second determination of Rs, n and Φ_{B}.

Rs values obtained from $\mathrm{d}V/\mathrm{d}\ln(I)$ with respect to I, as well as that obtained from the function $H(I)$, are 120 Ω and 130 Ω, respectively, in good agreement with each other. The average value is 125 Ω.

The values of Rs and n derived from curve $\mathrm{d}V/\mathrm{d}\ln(I)$ vs. I, and Rs and Φ_{B} obtained from the function $H(I)$ vs. I plot, are all included in Table 1.

To further reduce the dark current Is, we proposed different time of etching 5, 7 and 10 min, taking care to keep the thickness of the PSi as such.

Figure 6 shows the set of reverse I-V characteristics of PSi samples prepared at the same current density (1 mA/cm^2) with an etching time of 5, 7 and 10 min.

We observed that when the etching time increased, Is reduced to almost two orders of magnitude as it prepared for 5 min.

With the choice of an etching time of 5 min, 7 min and 10 min, we obtain a barrier height of 0.795 eV, 0.840 eV and 0.882 eV respectively.

Assuming that the temperature was kept constant, and referring to the relation ($Is \approx T^2 e^{-q\Phi_B/kT}$), the saturation current Is could be varied by the height of the barrier.

We assume that prolonged exposure of the silicon surface in HF etching varies the size of nanocrystallites which in turn modulates the band gap of the material.

According to the theory of Rhoderick and Williams [20], the band gap energy could be dependent on the height of the barrier Schottky contacts when there are enough of interface states. Consequently, the current undergoes a decrease following the equation (2).

To test these hypotheses: Rhoderick theory and the concept of quantum confinement are presented. We will first present, Rhoderick analysis to show the relationship between the barrier height Φ_B and the band gap energy. In the second step, we will use the concept of quantum confinement to express the energy of the band gap of PSi depending on the size of nano-crystallites.

The barrier height of the metal-semiconductor structure is generally determined by the work function of the semiconductor in addition to the energy level of the interface states. The general expression is described as follows:

$$q\Phi_B = \gamma(\Phi_m - \chi s) + (1-\gamma)(Eg - \Phi_0), \qquad (8)$$

where Φ_m is the work function of the metal, χ_S is the electron affinity of the semiconductor, and Φ_0 is the charge neutrality level value with respect to the bottom of the valance band at the surface of the semiconductor. The term γ is a parameter inverse of the well-known ideality factor, n; it is a measure of conformity of the diode to pure thermionic emission [21].

For an ideal Schottky diode, free density of interface states, $\gamma = 1$, the barrier height Φ_B approaches Schottky-Mott limit [22], which is $\Phi_B = q\Phi_m - q\chi_S$.

In contrast, in the presence of interface states, the case of Ni/PSi system makes the height of the barrier function of the energy of the band gap.

The expression of the barrier height is given by equation (8), and is close to the Bardeen limit [23]:

$$q\Phi_B = Eg^{(PSi)} - q\Phi_0, \qquad (9)$$

where $Eg^{(PSi)}$ is the energy gap of the PSi film and $q\Phi_0$ is the energy level of the interface state above the valence band. The Fermi level of the system metal/n-type semiconductor is often pinned, and $q\Phi_0$ for PSi is about $\approx Eg^{(PSi)}/3$ [24].

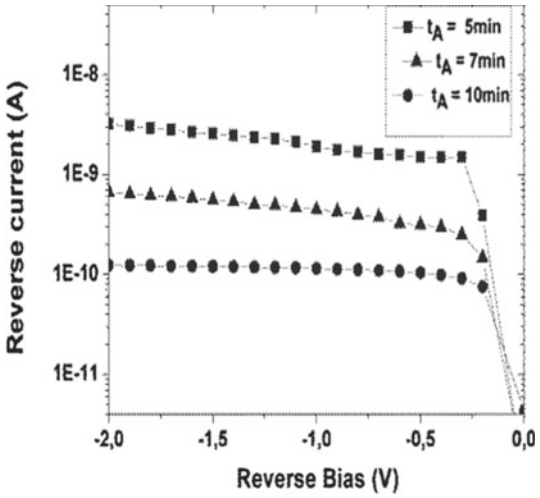

Fig. 6. Reverse *I-V* characteristics for MSM-PD device obtained with, current density of 1 mA/cm^2, HF concentration of 1% and an etching time of 5,7 and 10 min.

To clarify this theory, and considering that the system Ni/PSi/c-Si contains enough interface states between metal and PSi film, the barrier height should be related to the gap energy as seen in equation (9). The presence of enough interface states makes Φ_B independent or only weakly dependent on the work function of the metal. The same observations were reported for Cu/GaAs Schottky barrier prepared by anodization process [25].

Figure 7 shows clearly the formation of PSi layer and blue aspect of the layer. The observations were taken under room light. As reported the blue aspect was attributed to the presence of impurities within the oxide silicon that covers the nano-crystalline silicon [26]. The presence of the ambient air covers the freshly formed silicon nanowires.

For little variation of the anodization time, the aspect of the surface shows the blue and yellow colors, the surface becoming close to yellow for a time of 10 min.

For an etching time longer than 10 min, we see that the PSi film takes off from the surface, and the structure becomes more porous like that indicated in Figure 8.

Figure 9 shows the PL spectra of the PSi thin films at room temperature, recorded in the energy interval between 1.25 eV and 2.7 eV.

The excitation of the sample was carried out with He-Cd laser 325 nm.

The photoluminescence (PL) response showed a red band emission.

Table 1. The experimental values of some parameters obtained from *I-V* characteristics in low and high forward bias. $J = 1$ mA/cm^2, etching time: 5 min.

Electrical parameters	Barrier height (eV)	Ideality factor	Series resistance (Ω)
Low forward bias ($V < 0.7$ V)	0.794	1.03	neglected
High forward bias ($V > 0.7$ V)	0.810	3.83	125

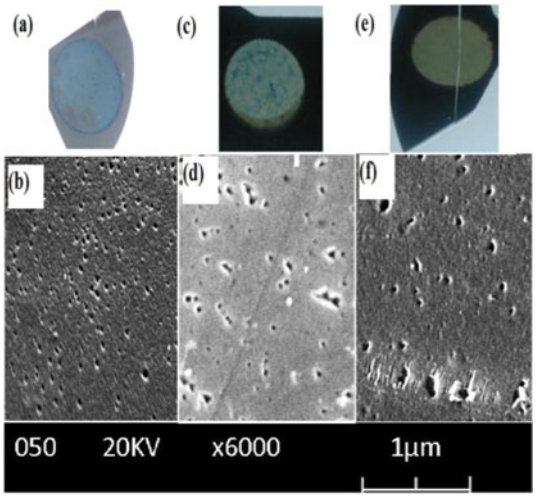

Fig. 7. SEM photograph of PSi top surface and color aspect of thin PSi layer recorded by Nikon Coolpix S620 camera, 5 min, 7 min and 10 min from left to right.

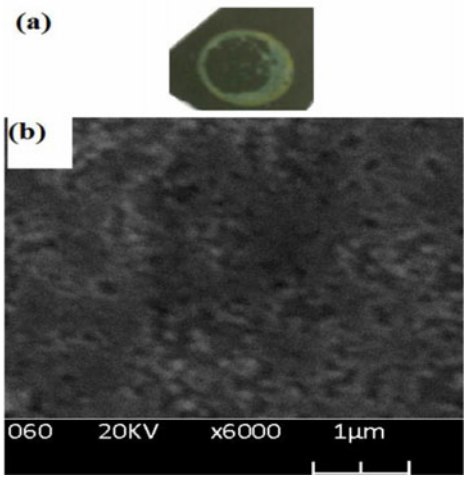

Fig. 8. (a) Presentation of sample with a longer etching time. Take off of PSi film after an etching time of 13 min recorded by Nikon Coolpix S620 camera. (b) SEM photograph of PSi top surface.

As was reported by Bessais et al., PL spectra were attributed to quantum confinement, considering the PSi film as a mixture of particles with spherical shaped nanocrystallites and quantum wires (QW), having different sizes [27]. According to the work reported in [28–30], the presence of nanocrystallites contributed to the existence of a broadband luminescence emission and wider energy band gap ranging from 1.8 to 2.6 eV.

These values are in good agreement with our experimental results (gap energy ranging 1.7–2 eV) and allow suggesting that PSi film is formed by nano-element particles.

Among the models describing the transport phenomena in the semiconductor nanostructure, the model of quantum confinement coupled with the approximation of the effective mass of charge carriers [31].

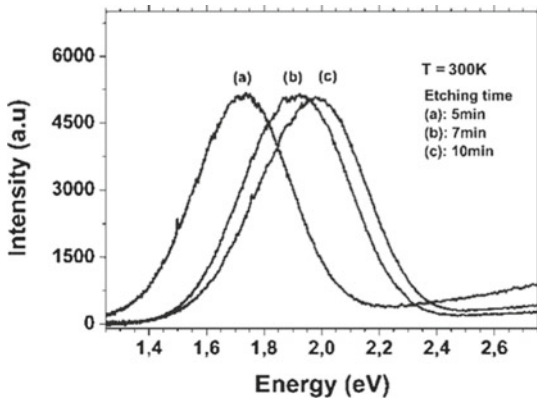

Fig. 9. Room temperature photoluminescence spectra of samples prepared with an etching time of 5, 7 and 10 min.

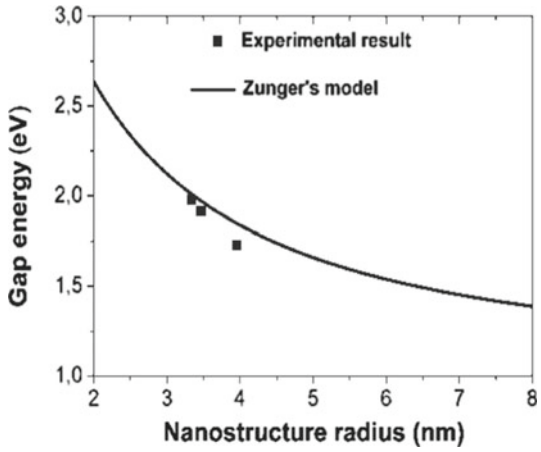

Fig. 10. Gap energy eVolution versus nano-element diameter R (nm).

The energy gap suffered by the presence of nanoporous silicon can be expressed as, $Eg^{(\mathrm{PSi})} = Eg^{(\mathrm{Si})} + \Delta E$, where $\mathrm{Eg}^{(\mathrm{Si})}$ is the potential energy of the electrons in the silicon of 1.12 eV.

Indeed, ΔE (eV) is the gap energy shift of the conduction and valence bands due to the quantum confinement of carriers inside the nanocrystallites.

When the structure is formed, electrons are confined in spheres of radius R (nm), and the shift is given as:

$$\Delta E = 2h^2/(m^* R^2), \tag{10}$$

here h is the Planck's constant (6.64×10^{-34} J s) and m^* is the effective mass of electron in the original silicon material. At 300 K, $m_e^* = 0.26\, m_0$ and $m_h^* = 0.40\, m_0$.

Figure 10 shows the comparison between, both the diameter deduced from equation (10) and that calculated by Zunger's model, whereas the nano-particles having as a finite size of the radius R (quantum dot) [32].

The nanostructures particles of radius R are close to those reported by Zunger's model, which allows us to say that the nanostructures particles tend to form spherical shapes.

In light of these models an explicit relationship between the saturation current Is and the size of

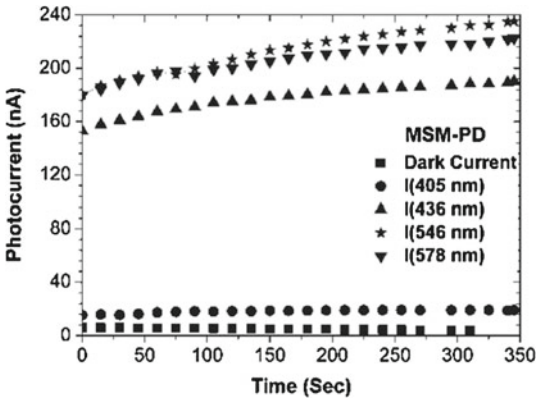

Fig. 11. Photoconductivity response spectra of MSM-PD device based on PSi film.

nano-element sizes can be deduced,

$$I\mathrm{s} = I\mathrm{s}^{(s_i)} \mathrm{e}^{-(2h^2/(m*R^2))/kT}, \tag{11}$$

where,

$$I\mathrm{s}^{(s_i)} = AA\ \mathrm{e}^{(q\Phi_0 - E_g^{(s_i)})/kT}. \tag{12}$$

Equation (11) is the combination of equations (9) and (10) showed above.

R is the radius of a nano-element of PSi films, h is the Planck constant and m^* is the effective mass of the electron. The suggested relationship between the dark current and a nano-element size of PSi structure explains the reduction of Is (Fig. 6). This relation explains clearly the decrease of Is due to the quantum effect.

Etching the silicon makes the nanostructured surface; the size of nano-element is characterized by an average radius R. The charge carriers are confined inside nano-elements.

As presented by PL measurements the band gap energy of silicon is shifted from bulk value of 1.12 eV to high value of 2 eV for PSi film.

Figure 11 shows the measured photocurrent of the MSM-PD device. The photocurrent is stable over a wide time interval. The photocurrent is maximum for the wavelength of 546 nm (2.27 eV) and quite pronounced for wavelengths of 578 nm and 436 nm. The diminution of high intensity of the photocurrent is observed for the wavelength of 405 nm which can be caused by a high reflection in the near UV spectra.

Photoconductivity of MMS-PD in the dark room had a current of 7 nA at a voltage of 1 V. Under illumination, the photocurrent reaches the value of 240 nA.

The illumination light is strongly absorbed by the PSi films supporting the creation of electron-hole pairs. The absorbed energy equivalent to 2.270 eV for the wavelength 546 nm is almost close to 1.979 eV bandgap of PSi determined by PL measurements.

4 Conclusion

The performance of the MSM-PD depends mainly on the barrier height of the Schottky contacts. We considered both MSM configuration and for comparison the Ni/PSi/c-Si conventional system. Both configurations confirm barrier height identical between the nickel and the porous silicon ($\Phi_B = 0.793$ eV), and a dark current of 3.1×10^{-9} A.

To further reduce the dark current of MSM-PD, we proposed different etching time 5 min, 7 min and 10 min, taking care to keep the thickness of the PS layer as well.

The dark current was reduced by almost two orders of magnitude for 10 min and dark current of $\approx 10^{-10}$ A.

Reducing the dark current is the result of the increase in the barrier height of 0.793 to 0.882 eV when the etching time is doubled to 10 min. We found that the height of the Schottky barrier depends on the gap of the material when the interface states are dominant. This confirmation was predicted by the theory of Rhoderick.

We found according to quantum theory applied to nanostructures PSi film, the size of nano-element coincided with Zunger's model. In addition, the height of the barrier depended explicitly on the size of the nanostructures.

The size of the nanostructures determined by equation (10) showed above is in good agreement with Zunger's model.

In light of these models, we suggest that the saturation current Is can be controlled by the size of nanocrystallites.

The practical method is to increase the etching time which in turn will reduce the size of the nanocrystallites. According to quantum theory this will bring back to increase the energy of the band gap of a term ΔE ($\Delta E = 2h^2/(m^*R^2)$).

Photosensitivity response is well established for the structure of PSi for the MSM-PD device. The dark current to a value of 7 nA, while the photocurrent under illumination is of the order of 240 nA.

This shows that the light can be effectively and strongly absorbed by the nanocrystalline structure of the PSi films.

References

1. B.L. Szentpali, T. Mohacsy, I. Barsony, Curr. Appl. Phys. **6**, 174 (2006)
2. Y. Zhao, D.-S. Li, J. Zhao, W.-B. Sang, D.-R. Yang, M.-H. Jiang, Curr. Appl. Phys. **8**, 206 (2008)
3. V.V. Iyengar, B.K. Nayak, M.C. Gupta, Solar Energy Mater. Solar Cells **94**, 2251 (2010)
4. M. Ben Rabha, B. Bessais, Sol. Energy **84**, 486 (2010)
5. M. Rajabi, R.S. Dariani, J. Porous Mater. **16**, 513 (2009)
6. J. Torres, H.M. Martinez, J.E. Alfonso, L.D. Lopez C., Microelectronics **39**, 482 (2008)
7. R.S. Dubey, D.K. Gautam, Opt Quant. Electron **41**, 189 (2009)
8. Z. Ben Achour, O. Touayar, E. Akkari, J. Bastie, B. Bessais, J. Ben Brahim, Nucl. Instrum. Methods Phys. Res. A **579**, 1117 (2007)

9. M. Bakir, C. Chui, A. Okyay, K. Sarawast, J. Meindi, IEEE Trans. Electron Devices **51**, 1084 (2004)
10. M. Siegert, M. Loken, C. Glingener, C. Buchal, IEEE J. Sel. Top. Quantum Electron. **4**, 97 (1998)
11. F. Xie, H. Lu, X.Q. Xiu, D.J. Chen, P. Han, R. Zhang, Y.D. Zheng, Solid-State Electron. **57**, 39 (2011)
12. N.N. Jandow, E.K. Yam, S.M. Thahab, H. Abu Hassan, K. Ibrahim, Curr. Appl. Phys. **10**, 1452 (2010)
13. Md. Nazrul Islam, S.K. Ram, S. Kumar, J. Phys. D: Appl. Phys. **40**, 5840 (2007)
14. H. Khalili, R.S. Dariani, A. MortezaAli, V. Daadmehr, K. Robbie, J. Mater. Sci. **42**, 908 (2007)
15. A.F. Abd Rahim, M.R. Hashim, N.K. Ali, Physica B **406**, 1034 (2011)
16. I.M. Afandiyeva, I. Dokme, S. Altindal, L.K. Abdullayeva, S.G. Askerov, Microelectron. Eng. **85**, 365 (2008)
17. S.M. Sze, K.K. Ng, *Physics of Semiconductor Devices*, 3rd edn. (John Wiley & Sons, Inc., 2007), p. 179
18. D. Korucu, T.S. Mammadov, S. Ozcelik, J. Ovonic Res. **4**, 159 (2008)
19. S.K. Cheung, N.W. Cheung, Appl. Phys. Lett. **49**, 85 (1986)
20. E.H. Rhoderick, R.H. Williams, *Metal Semiconductor Contacts* (Clarendon Press, Oxford, UK, 1988), pp. 20, 48, 99
21. H.C. Card, E.H. Rhoderick, J. Phys. **4**, 1589 (1971)
22. N.F. Mott, Proc. Cambridge Philos. Soc. **34**, 568 (1938)
23. J. Bardeen, Phys. Rev. **71**, 717 (1947)
24. S.M. Sze, K.K. Ng, *Physics of Semiconductor Devices*, 3rd edn. (John Wiley & Sons, Inc., 2007), p. 142
25. M. Biber, A. Turut, J. Electron. Mater. **31**, 1366 (2002)
26. L. Tsybeskov, Ju.V. Vandyshe, P.M. Fauchet, Phys. Rev. B **49**, 7821 (1994)
27. B. Bessais, H. Ezzaouia, M.F. Boujmil, O. Ben Younes, H. Elhouichet, A. Chihi, J. Porous Mater. **7**, 311 (2000)
28. L.T. Canham, Appl. Phys. Lett. **57**, 1046 (1990)
29. V. Lehmann, U. Gosele, Appl. Phys. Lett. **58**, 856 (1991)
30. J. Anto Pradeep, P. Gogoi, P. Agarwal, J. Non-Cryst. Solids **354**, 2544 (2008)
31. D.J. Lockwood, P. Schmuki, H.J. Labbé, J.W. Fraser, Physica E: Low-Dimens. Syst. Nanostruct. **4**, 102 (1999)
32. A. Zunger, L.-W. Wang, Appl. Surf. Sci. **102**, 350 (1996)